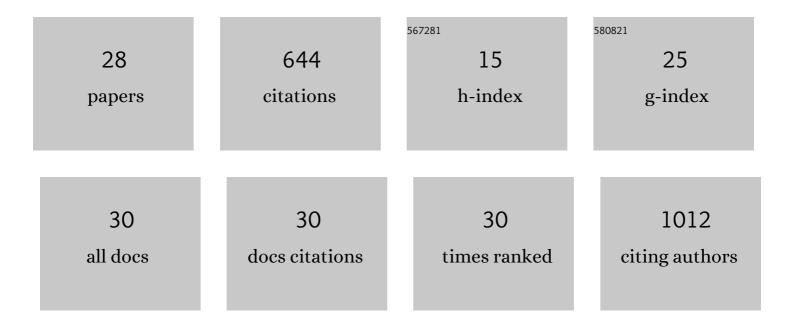
## TomÃ;Å; PluhÃ;Äek

List of Publications by Year in descending order

Source: https://exaly.com/author-pdf/5944884/publications.pdf Version: 2024-02-01



#	Article	IF	CITATIONS
1	Ultra-trace determination of oxaliplatin impurities by sweeping-MEKC-ICP-MS. Microchemical Journal, 2022, 172, 106967.	4.5	4
2	Climate change extreme and seasonal toxic metal occurrence in Romanian freshwaters in the last two decades—case study and critical review. Npj Clean Water, 2022, 5, .	8.0	17
3	Tutorial and spreadsheet for the evaluation of instrumental quantification uncertainty by the linear weighted regression model: Determination of elemental impurities in a nasal spray by ICP-MS. Talanta, 2021, 225, 122044.	5.5	7
4	Freeing Aspergillus fumigatus of Polymycovirus Infection Renders It More Resistant to Competition with Pseudomonas aeruginosa Due to Altered Iron-Acquiring Tactics. Journal of Fungi (Basel,) Tj ETQq0 0 0 rgl	BT /Ovæ <b>s</b> lock	10115 50 617
5	Noninvasive Combined Diagnosis and Monitoring of Aspergillus and Pseudomonas Infections: Proof of Concept. Journal of Fungi (Basel, Switzerland), 2021, 7, 730.	3.5	11
6	Evidence of declining trees resilience under long term heavy metal stress combined with climate change heating. Journal of Cleaner Production, 2021, 317, 128428.	9.3	18
7	Study of interactions between carboxylated core shell magnetic nanoparticles and polymyxin B by capillary electrophoresis with inductively coupled plasma mass spectrometry. Journal of Chromatography A, 2020, 1609, 460433.	3.7	9
8	Past and present anthropic environmental stress reflect high susceptibility of natural freshwater ecosystems in Romania. Environmental Pollution, 2020, 267, 115505.	7.5	13
9	Measurement uncertainty evaluation from correlated validation data: Determination of elemental impurities in pharmaceutical products by ICP-MS. Talanta, 2020, 220, 121386.	5.5	14
10	Rhizoferrin Glycosylation in Rhizopus microsporus. Journal of Fungi (Basel, Switzerland), 2020, 6, 89.	3.5	10
11	lon-exchange HPLC-ICP-MS: A new window to chromium speciation in biological tissues. Talanta, 2020, 218, 121150.	5.5	21
12	A direct LA-ICP-MS screening of elemental impurities in pharmaceutical products in compliance with USP and ICH-Q3D. Analytica Chimica Acta, 2019, 1078, 1-7.	5.4	19
13	Determination of oxaliplatin enantiomers at attomolar levels by capillary electrophoresis connected with inductively coupled plasma mass spectrometry. Talanta, 2019, 205, 120151.	5.5	18
14	Myocardial iron homeostasis and hepcidin expression in a rat model of heart failure at different levels of dietary iron intake. Biochimica Et Biophysica Acta - General Subjects, 2019, 1863, 703-713.	2.4	20
15	Analysis of Microbial Siderophores by Mass Spectrometry. Methods in Molecular Biology, 2019, 1996, 131-153.	0.9	5
16	Recent advances in chromium speciation in biological samples. Spectrochimica Acta, Part B: Atomic Spectroscopy, 2019, 152, 109-122.	2.9	25
17	Content of distinct metals in periprosthetic tissues and pseudosynovial joint fluid in patients with total joint arthroplasty. Journal of Biomedical Materials Research - Part B Applied Biomaterials, 2019, 107, 454-462.	3.4	10
18	Study of chromium species release from metal implants in blood and joint effusion: Utilization of HPLC-ICP-MS. Talanta, 2018, 185, 370-377.	5.5	17

TomÃiÅi PluhÃiÄek

#	Article	IF	CITATIONS
19	Early and Non-invasive Diagnosis of Aspergillosis Revealed by Infection Kinetics Monitored in a Rat Model. Frontiers in Microbiology, 2018, 9, 2356.	3.5	23
20	Laser ablation inductively coupled plasma mass spectrometry imaging: A personal identification based on a gunshot residue analysis on latent fingerprints. Analytica Chimica Acta, 2018, 1030, 25-32.	5.4	15
21	Membrane depolarization and aberrant lipid distributions in the neonatal rat brain following hypoxic-ischaemic insult. Scientific Reports, 2018, 8, 6952.	3.3	10
22	Batch-processing of imaging or liquid-chromatography mass spectrometry datasets and De Novo sequencing of polyketide siderophores. Biochimica Et Biophysica Acta - Proteins and Proteomics, 2017, 1865, 768-775.	2.3	20
23	Biodistribution of upconversion/magnetic silica-coated NaGdF <sub>4</sub> :Yb <sup>3+</sup> /Er <sup>3+</sup> nanoparticles in mouse models. RSC Advances, 2017, 7, 45997-46006.	3.6	21
24	Ultra-high performance supercritical fluid chromatography-mass spectrometry procedure for analysis of monosaccharides from plant gum binders. Analytica Chimica Acta, 2017, 989, 112-120.	5.4	27
25	Non-invasive and invasive diagnoses of aspergillosis in a rat model by mass spectrometry. Scientific Reports, 2017, 7, 16523.	3.3	23
26	Myocardial iron content and mitochondrial function in human heart failure: a direct tissue analysis. European Journal of Heart Failure, 2017, 19, 522-530.	7.1	180
27	Characterization of microbial siderophores by mass spectrometry. Mass Spectrometry Reviews, 2016, 35, 35-47.	5.4	61
28	<i>Aspergillus</i> infection monitored by multimodal imaging in a rat model. Proteomics, 2016, 16, 1785-1792.	2.2	13